Regular Article

PHYSICAL CHEMISTRY RESEARCH
Published by the
*Iranian Chemical Society*
www.physchemres.org
info@physchemres.org

***Phys. Chem. Res.**, Vol. 6, No. 3, 463-478, September 2018*
**DOI: 10.22036/pcr.2018.119027.1469**

# Theoretical Study on Structure and Electronic Properties of Aniline-5-Membered Heterocyclic Co-oligomers

A. Dadras, M.R. Nateghi* and F. Kalantari-Fotooh
*Department of Chemistry, Yazd Branch, Islamic Azad University, Yazd, Iran*
*(Received 18 February 2018, Accepted 24 April 2018)*

With the aim of exploring the electronic and optical properties of some interesting conductive copolymers in view of potential applications, a regular oligomer systems made of aniline and three reference heterocyclic compounds (pyrrole, thiophene and furan) are studied using density functional theory (DFT) and time dependent DFT (TDDFT) calculations at B3LYP/6-31+G(d,p) level. It was found that poly (aniline-co-pyrrole) has the lowest ionization potential (4.48 eV) and electro affinity (0.77 eV) while poly (aniline-co-thiophene) has the lowest band gap and longest (3.21 eV) wavelength of absorption (and therefore the highest electronic conjugation) among the studied molecules. Comparison of the theoretical data and spectroscopic results obtained by DFT calculations with those experimentally obtained show very good agreement.

**Keywords:** Aniline, Density functional theory, Furan, Band gap, Conducting polymers

## INTRODUCTION

Conducting polymers have been subjected to the numerous investigations because their unique properties make them suitable in various scientific and industrial applications such as optical and electronic devices, sensors, corrosion protection, microelectronic devices solar cells, fuel cells and supercapacitors [1-10].

A large number of theoretical and experimental research activities have been devoted to conjugated polymers such as polythiophene, polyEDOT, polyfuran and polyaniline, due to their ease of synthesis, good doping dedoping chemistry, environmental stability and low cost of their monomer [11-17]. However, increasing demands on new materials with desired properties has motivated scientists to develop polymers having a collection of given properties [18-28]. Copolymerization is an efficient way to get enhanced physical, electronic and mechanical properties relative to the individual homo polymers [29-33]. Li *et al.* reported broad conductivity values for aniline/furan random copolymers [34]. Aniline and pyrrole were efficiently copolymerized and used as a substrate for the immobilized cholesterol oxidase film in order to prepare a biosensor [35]. Aniline-thiophene copolymer is very interesting, because its oxidized form is completely stable even at high electrode potentials [36-39]. The random copolymerization of aniline and thiophene with varying concentration ratios was studied in acetonitrile by Holz *et al.* [36,38]. Thiophene and furan are not soluble in water and their oxidation potentials are higher than that of aniline. Therefore, random copolymerization of these very famous monomers should be performed in non-aqueous solutions. Moreover due to the very higher oxidation potentials, thiophene and furan participate in random copolymer formation process much less than aniline. So, the formed copolymer chains are rich of aniline moieties. To overcome these difficulties, three new monomers containing thiophene, furan or EDOT and aniline were synthesized by Nateghi *et al.* [31-33]. These monomers were soluble in water and could be polymerized into regular polymers. The thin layer of these copolymers exhibit corrosion protection effects on steel electrode in comparison with corresponding polyaniline and polyfuran

*Corresponding author. E-mail: mnateghi@iauyazd.ac.ir

homopolymers.

Density functional theory (DFT)-based calculations have been significant in understanding electronic properties of different systems in atomic scale [40,41]. The DFT approach is also commonly used to determine properties of conjugated systems [42-44]. Therefor, performing studies using DFT will aid experimentalists in the design, prediction and functionalization of different materials necessary for a specific application. Thiophene based copolymers were the subject of many theoretical studies [5, 6,45-47]. Zgou et al. have been combined DFT calculations with experimental results on thiophene-phenylene co-oligomer to propose an oligomer model by examining the initiating and propagation reaction. They also investigated the effect of alkyl and alkoxy groups on various properties of copolymer [5]. DFT calculations were also applied to study the structure and electronic properties of oligomers based on bithiophene, bifuran and bipyrrole bridged by $sp^2$ carbon substituted by CO, S, Se and Te atoms [26]. The results showed that insertion of a bridging group leads to reduction of the HOMO-LUMO energy gap. The bridging effect on oligothiophene with some organic functional groups was investigated by Hamidi *et al.* [46]. Recently, a great attention was devoted to thiophene-containing polymers in order to be employed in fabrication of polymer solar cells [6,47]. Tsinge *et al.* investigated the effect of heteroatoms on structural and electronic properties of some thiophene based conjugated polymer. They found that oxygen derivatives give rise to increase charge dissociation and are more applicable in polymer solar cells [47]. Franco *et al.* showed that fluorine substituted conjugated oligomers may lead to solar cells with improved conversion efficiency [6]. Two thiophene-fluorine based copolymers were studied by the DFT method to inquire their applicability as efficient photo luminescent solid film substances [45]. However, there are little theoretical literatures on pyrrole and furan based copolymers [48-50]. Kamran *et al*. investigated the structure and conductivity of an oligomer consisting of aniline and pyrrole through comparison of experimental and theoretical calculations containing three aniline and three pyrrole units [48]. DFT calculations were also performed for investigating the HOMO-LUMO energy gap of 4,7-di(furan-2-yl)benzo [29,51] selenadiazole conjugated polymer for polymeric solar cell applications [49]. The neutral and dicationic states of eight conjugated oligomers containing thiophenes and pyrrole rings were studied by Fomine *et al.* [50]. Therefore, based on what literature review indicates there is a great interest in theoretical and experimental studies on the conjugated polymers since of their widespread applications in various aspects of human life.

In the present work, we theoretically investigate the structure, electronic and optical properties of regular copolymers based on aniline and heterocyclic compounds from newly synthesized respecting comonomers using DFT calculations. The results are compared with those experimentally obtained by our group. The oligomerization mechanism is investigated and the best situation for inserting next monomers in progression steps is selected by spin density results. TD-DFT calculations are performed for UV-Vis spectra and optical band gap calculations.

## COMPUTATIONAL DETAILS

All calculations are performed using Gaussian 09 program [52] and the results are visualized through GaussView [53]. The geometry of monomers, dimers and co oligomers of aniline-thiophene (PAT), aniline-pyrrole (PAP) and aniline-furrane (PAF) and their radical cation structures are fully optimized using density functional theory (DFT) at the B3LYP level and 6-31+G(d,p) basis set. Then, the frequency calculations are performed for all species on the optimized structures, using the same theory. In order to evaluate the energy gap as the difference between the HOMO and LUMO levels their respecting energies are computed. The spin density populations are investigated for predicting the polymerization mechanism. IR spectra are simulated and scaled with a common scaling factor of 0.9613 [54]. The UV-Vis spectra are simulated at TD-DFT-B3LYP/6-31G** level of theory. All calculations are performed in gas phase, except UV-Vis spectra which is simulated in DMSO medium, using polarized continuum model (PCM).

## RESULTS AND DISCUSSION

### Oligomerization Mechanism

A schematic reaction path of the oligomerization

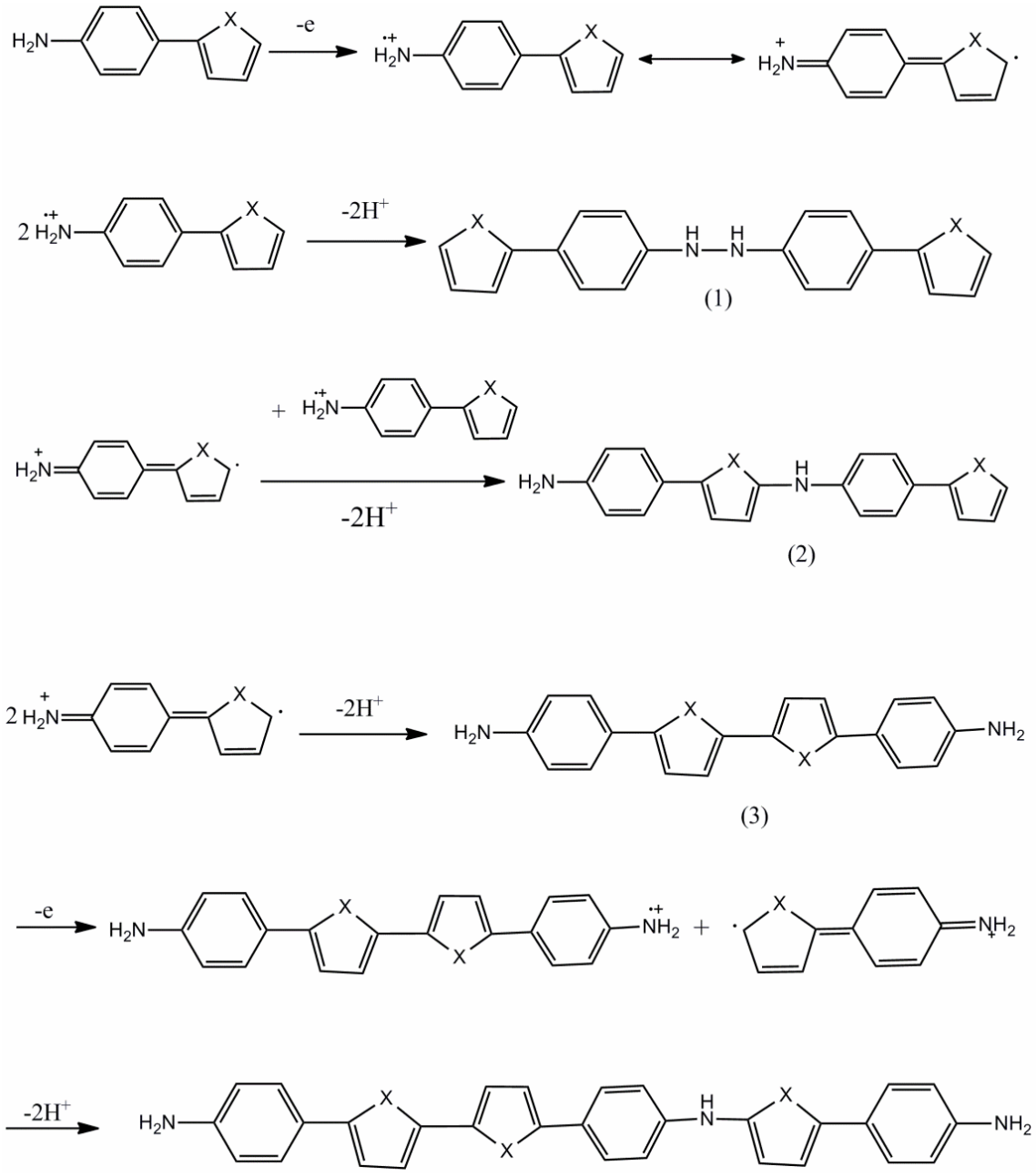


**Fig. 1.** A schematic reaction path of the oligomerization mechanism of the studied molecules.

mechanism [5] of aniline-thiophene (PAT), aniline-pyrrole (PAP) and aniline-furan (PAF) are proposed in Fig. 1. Table 1 shows the natural charges calculated using NBO analysis of neutral co-oligomers. The results show that N atoms of anilines carry the highest electron accumulation. So, at the first step of the polymerization reaction, one electron is removed from $NH_2$. There are three probabilities for bonding the monomer to each other, (1) (2) and (3) in the Fig. 1. The spin density population of each atom of the respecting radical cations and dimers are presented in Table 2. The results show that the highest spin density is related to the carbon atom near the heteroatom in heterocycle ring.

**Table 1.** Natural Charge of Neutral Monomers Calculated Using NBO Analysis. The Numbers of Atoms are Presented in the Figure Bellow

| | C1 | C2 | C3 | C4 | C5 | C6 | C7 | C8 | X | N |
|---|---|---|---|---|---|---|---|---|---|---|
| PAT | -0.283 | -0.283 | -0.455 | -0.200 | -0.287 | 0.164 | -0.287 | -0.192 | 0.4340 | -0.870 |
| PAP | -0.309 | -0.325 | -0.0879 | -0.218 | -0.282 | 0.153 | -0.280 | -0.200 | -0.559 | -0.870 |
| PAF | -0.326 | -0.335 | 0.0787 | -0.199 | -0.284 | 0.158 | -0.284 | -0.196 | -0.464 | -0.867 |

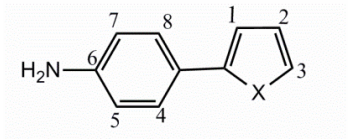


**Table 2.** The Spin Density Population of Each Atom of the Respecting Radical Cations and Dimers

| a | C1 | C2 | C3 | C4 | C5 | C6 | C7 | C8 | X | N |
|---|---|---|---|---|---|---|---|---|---|---|
| PAT | 0.204 | -0.0624 | 0.293 | -0.0197 | 0.0825 | 0.0995 | 0.0666 | -0.014 | -0.0424 | 0.195 |
| PAP | 0.1268 | -0.0141 | 0.314 | 0.007 | 0.147 | 0.107 | 0.0322 | 0.0227 | -0.0378 | 0.171 |
| PAF | 0.1883 | -0.0587 | 0.304 | -0.0283 | 0.0808 | 0.0960 | 0.0695 | -0.0020 | -0.0190 | 0.191 |

| b | C1 | C2 | C3 | C4 | C5 | C6 | C7 | C8 | C9 | C10 | N1 | N2 |
|---|---|---|---|---|---|---|---|---|---|---|---|---|
| 2PAT | -0.0634 | 0.131 | 0.066 | 0.146 | -0.066 | -0.066 | 0.15 | 0.0658 | 0.131 | -0.063 | 0.240 | 0.240 |
| 2PAP | -0.0150 | 0.0725 | 0.083 | 0.109 | -0.0270 | -0.0270 | 0.109 | 0.0830 | 0.0725 | -0.015 | 0.228 | 0.228 |
| 2PAF | -0.0291 | 0.0981 | 0.075 | 0.121 | -0.0471 | -0.0471 | 0.121 | 0.0754 | 0.0981 | -0.029 | 0.242 | 0.242 |

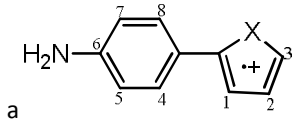


a

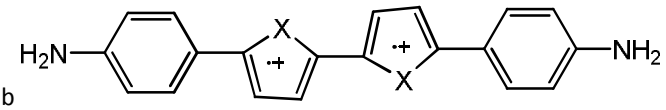


b

According to the charge density population of each atom (Table 2), C3 atoms of all radical cations have the highest spin density, so, the formed radical cations are bonded to each other through C3 atom near the electronegative heteroatom to form the dimmer (3). The C3 atom carriers unpaired electron π-spin density and is the most reactive site for dimer formation. On the other hand, the highest spin density for the trimmer formation and continuing polymerization can be attributed to nitrogen atom of aniline moiety.

The polymerization process can be continued in the same reactivity protocol. The progression step consists of the dimmer oxidation to produce radical reactions, coupling the radical cations and deprotonation until the final polymer is obtained. We stopped at the stage of six aromatic rings step for the reason of computational cost and the fact that by increasing the number of repeating units the electronic properties convergence occurs [23,28]. It has been shown

PAT

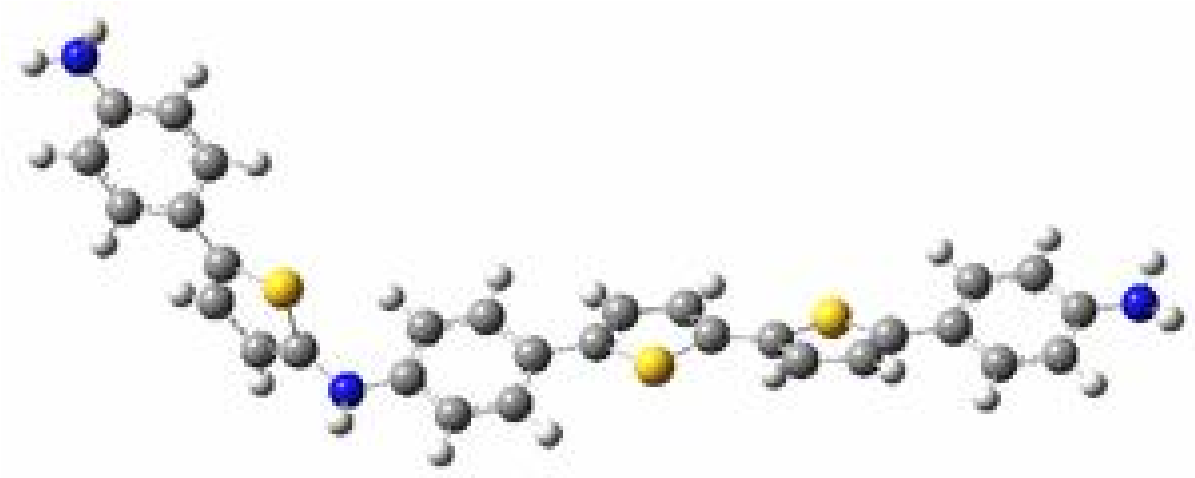

PAP

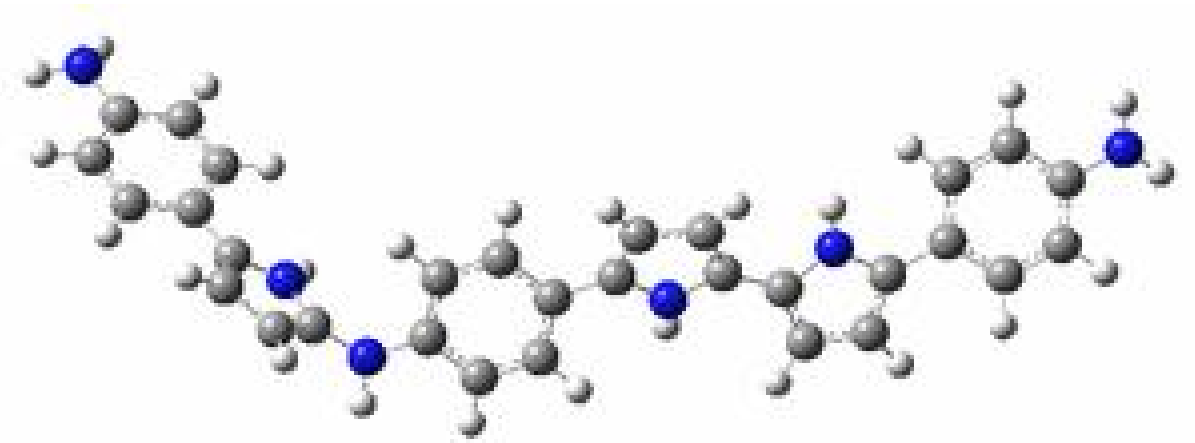

PAF

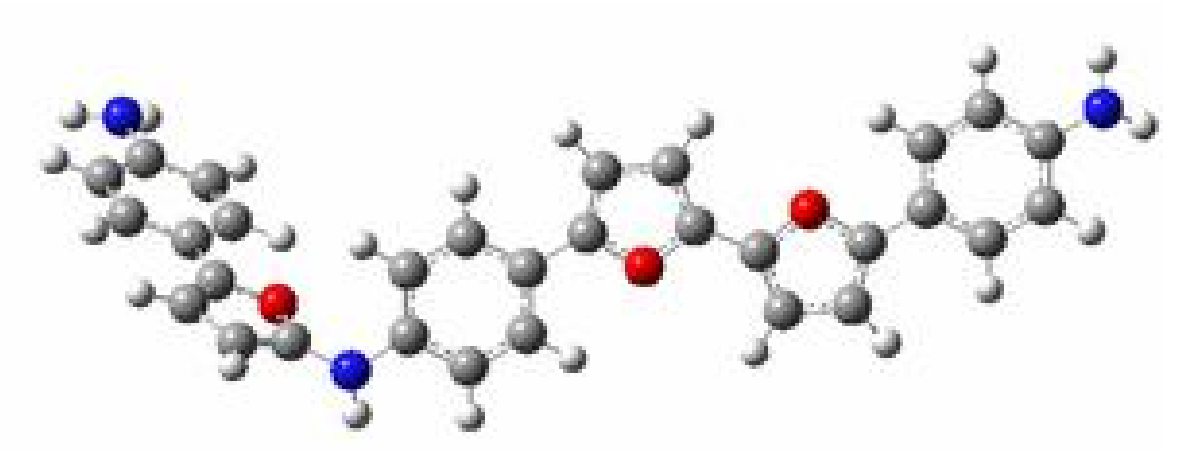

**Fig. 2.** The optimized structure of the studied molecules. Gray, blue, red and yellow balls stand for C, N, S and O atoms, respectively.

**Table 3.** Bond Lengths (A°) and Torsion Angles (Degree) of the Studied Oligomers

| C12-N11 | C14-C15 | C24-C26 | C19-C21 | C19-X20 | C16-C17 |
|---|---|---|---|---|---|
| 1.40 | 1.41 | 1.46 | 1.45 | 1.76 | 1.38 |
| 1.40 | 1.41 | 1.45 | 1.43 | 1.37 | 1.39 |
| 1.40 | 1.41 | 1.45 | 1.43 | 1.37 | 1.38 |
| 27-26-24-23 | 22-21-19-20 | 20-16-15-14 | 12-11-9-8 | 10-6-5-4 | - |
| 28.66 | -8.48 | -26.54 | 102.06 | 29.61 | - |
| -25.34 | -23.57 | 26.36 | 92.86 | -26.69 | - |
| -0.11149 | -0.06726 | 0.0498 | -111.54 | -3.250 | - |

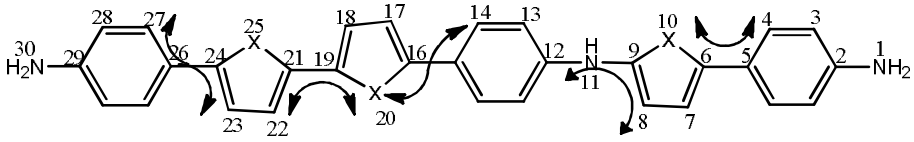

that for poly thiophene, the HOMO-LUMO energies convergence is achieved at around n = 8 [55,56], while for PCDTBT and PTB7, the convergence of the HOMO-LUMO energies is respectively achieved at n = 3 [57] and n = 4 [55], and for most donor acceptor copolymers it is at n = 4-6 [58].

## Structural Properties

The trimmer structures of neutral and radical cation forms of PAT, PAP and PAF were set in anti-configuration and let the structures to fully optimize using B3LYP/6-31+G(d,p) method. The optimized structures are shown in Fig. 2. All these geometries are in good twisted manner to minimize steric hindrance of hydrogen atoms. The bond lengths and dihedral angles are presented in Table 3. The results show that in PAT the torsional angle between aniline plane attached at para position to thiophene is about 26-30° including 1.46 Å inter ring distances. The torsional angle between two thiophene rings is -8.48° with 1.45 Å inter ring distance. A high torsional angle (102.06°) can be observed between the thiophene rings that is attached to N atom of aniline. The torsional angle between aniline and pyrrole in PAP is lower than that of PAP (about 25-26°) with 1.46 Å inter ring distance, which is due to the higher conjugation of aniline with pyrrole compared to thiophene. The torsional angle between two pyrrole ring is higher (23.57°) with the same inter ring distance. The torsional angle between the pyrrole and aniline bonded to the *N* atom is 92.86°.

In PAF the inter ring torsional angle are much lower than two other oligomers which are about 0.049-3° and -0.06726° for aniline-furan and furan-furan rings, respectively. This can be attributed to the lower atomic radius of O atom compared to S and N atoms. So, the higher conjugation between these rings is expected. The highest torsional angle (111.54°) can be observed between the furan rings attached to *N* atom of aniline.

## Electronic Properties of Oligomers

Table 4 shows the HOMO and LUMO energies, ionization potentials (IP) and electron affinity (EA) of three co-oligomers. Negative HOMOs and LUMOs are taken as IP and EA respectively, using Koopman's theorem. Contours of HOMOs and LUMOs are depicted in Fig. 3. The high number of atoms and the non-planarity of oligomers prevent the delocalization of electron density of HOMO and LUMO over the entire frame. Figure 3 shows that LUMO isosurfaces are diffused over inter ring bonds

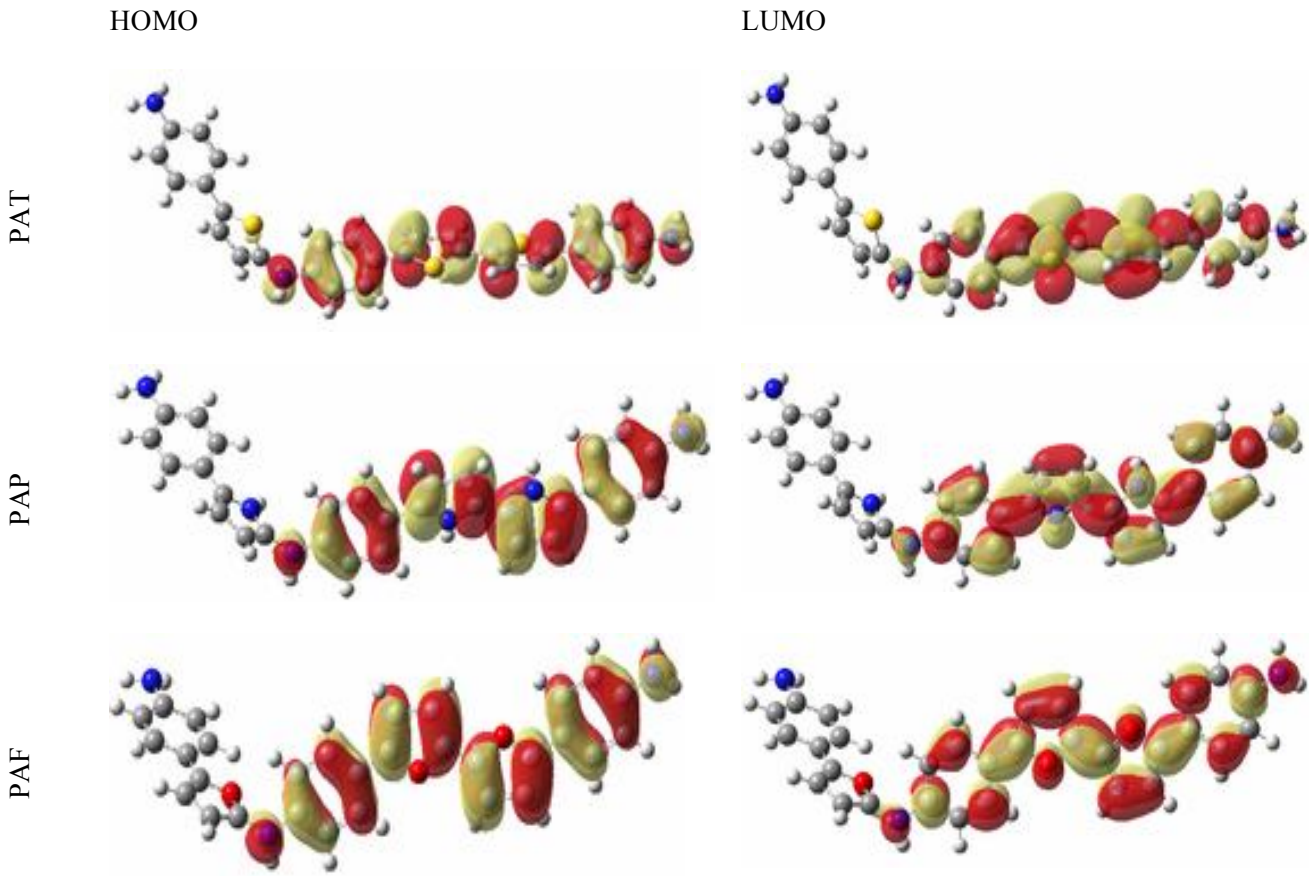


**Fig. 3.** Frontier orbitals at isovalue = 0.02 of PAT, PAP and PAF co-oligomers.

but HOMOs are mostly concentrated on the rings.

The results depicted in Table 4 show that PAP has the lowest IP and EA among the studied molecules. This structure has the highest torsional angels and is more twisted. So, the energy levels increase and results in less conjugation.

The HOMO-LUMO gaps ($E_g^{hl}$) and the lowest singlet excited energies $E_g^{opt}$ are both listed in Table 4. The computed values of $E_g^{opt}$ represent the vertical excitation energies from the ground state to the first excited state and are directly comparable to the optical band gap observed from UV-Vis absorption spectroscopy [18,31,33,48]. The computed values of $E_g^{hl}$ represent the valence to conduction band energy difference in the ground state and are directly comparable to the band gap measured from cyclic voltammetry. The available experimental values of $E_g^{opt}$ and $E_g^{hl}$ are also included in Table 4 for comparison. The results show that $E_g^{hl}$ values are all greater than the $E_g^{opt}$ values science it takes additional energy to fully separate electrons and holes into free carriers [6].

The difference in $E_g^{hl}$ and $E_g^{opt}$ is called the exciton binding energy ($E_B$). The largest $E_B$ was observed for PAP with large deviation from planarity. The results show that the calculated band gap of these co-oligomers are wider compared to those of homopolymers calculated by B3LYP/6-31G* method (2.41 eV for thiophene [59], 3.5 eV for pyrrole [60] and 2.81 eV for furan [26]). So, copolymerization of these heterocyclic compounds with aniline increases their band gap. Furthermore, results show that PAP has the broadest band gap and the band gap of PAT is smaller than those of two other oligomers, indicating its better π-conjugated structure. The narrow band gap could lead to the long wavelength absorption and emission. The calculated absorption $\lambda_{max}$ values of the three

**Table 4.** Gibbs Free Energies (G), HOMO-LUMO Energies, IP, EA, Calculated and Experimental [31,33,48] $E_g^{hl}$, $E_g^{opt}$, $E_B$, $\lambda_{max}$ and Oscillation Straight (O.S) of PAT, PAP and PAF

| Name | PAT | PAP | PAF |
|---|---|---|---|
| G (kJ) | -6604636.384 | -3904233.943 | -4060723.442 |
| HOMO (eV) | -4.8246 | -4.48144 | -4.6289 |
| LUMO (eV) | -1.6193 | -0.7665 | -1.3056 |
| IP (eV) | 4.8246 | 4.48144 | 4.6289 |
| EA (eV) | 1.6193 | 0.7665 | 1.3056 |
| $E_g^{hl}$ (eV) | 3.21 | 3.71 | 3.32 |
| $E_g^{hl}$ (exp) | - | - | 3.47 |
| $E_g^{opt}$ (eV) | 2.97 | 3.43 | 3.11 |
| $E_g^{opt}$ (exp) | - | 2.40 | 3.36 |
| $E_B$ (eV) | 0.24 | 0.28 | 0.21 |
| $\lambda_{max}$ (nm) | 416.07 | 360.94 | 398.04 |
| O.S | 1.6382 | 1.6395 | 1.6996 |

oligomers together with their oscillation straight are presented in Table 4. Among the studied molecules, PAT has the longest wavelength and so the most electronic conjunction.

## UV-Vis Spectral Characteristics

The theoretically simulated UV-Vis spectra of PAT, PAF and PAP co-oligomers at TD-DFT-B3LYP/6-31G** level of theory are given in Fig. 4.

The simulated UV-Vis spectrum of PAF shows two peaks at 415 ($\lambda_{max}$) and 305 nm, which are assigned to π-π* transition of benzenoid rings which are in close agreement with experimental results (390 and 305 nm) [31]. The other peaks are related to inter-band transition. In PAT oligomer, the peak concerned to π-π* transition shows a bathochromic shift toward wavelength 436 ($\lambda_{max}$), 318 and 309 nm. This can be attributed to the increase in conjugation. These results show correlations with experimental data peaks around 310 and 388 nm [33]. The UV-Vis spectrum of PAP shows hypsochromic shift in π-π* transition to 367 ($\lambda_{max}$) and 289 nm which is due to the transition of valence electron to the conduction band. The experimental π-π* value reported for aniline-co-pyrrole is 324 nm [61]. So, PAP has the lowest conjugation compared with other structure which can be attributed to its higher twisted structure.

## Infra-red Spectroscopy

The theoretically simulated IR spectra of PAT, PAP and PAF oligomers of three repeating units are given in Fig. 5. These spectra are calculated by B3LYP/6-31+G** method and the systematic errors in calculations are removed by applying a scaling factor of 0.9613 [52,54]. The major peak values of three conjugated oligomers along with their experimental bands are given in Tables 5-7. For PAT, the calculated 3441 $cm^{-1}$ and 3452 $cm^{-1}$ bands are assigned to N-H stretching, 3086 $cm^{-1}$ is assigned to C-H thiophene ring asymmetric stretching, and 3049-3069 $cm^{-1}$ are assigned to C-H of aniline ring. The difference in simulated and observed N-H stretching can be attributed to the fact that

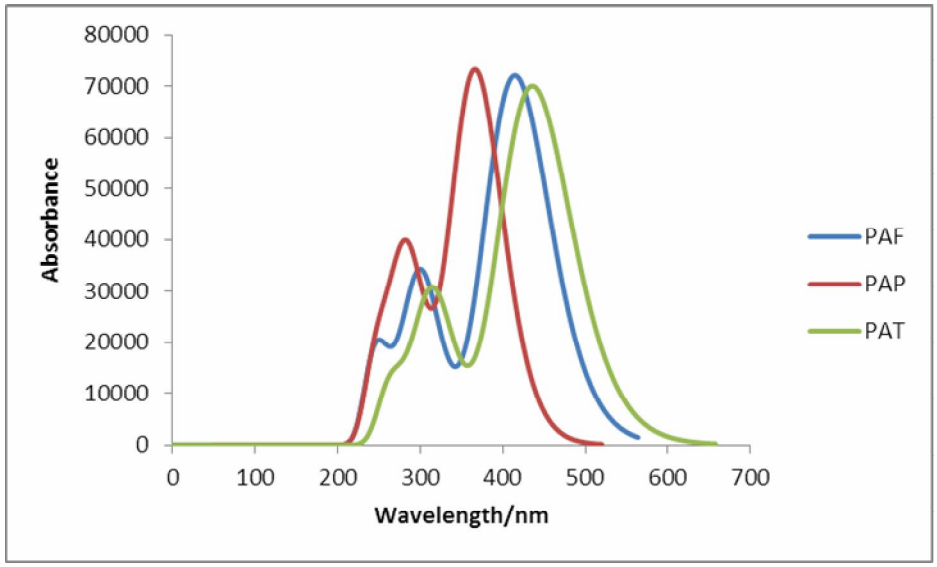


**Fig. 4.** simulated UV-Vis spectra of PAF, PAP and PAT co-oligomers.

**Table 5.** Experimental and Calculated Frequencies (in $cm^{-1}$) of PAT

| No. | Calculation frequency | | Experimental [33] | Approximate assignment |
|---|---|---|---|---|
| | Unscaled | Scaled | | |
| 1 | 3580-3687 | 3441-3544 | - | ν N-H (Ani ring) |
| 2 | 3591 | 3452 | 3440 | ν N-H (Bridging) |
| 3 | 3210 | 3086 | - | ν C-H (Thiophene ring) |
| 4 | 3172,3193 | 3049-3069 | - | ν C-H (Ani ring) |
| 5 | 1671-1659 | 1606-1595 | - | ν C=C (Ani ring), wag N-H |
| 6 | 1605 | 1543 | - | ν C=C (Thiophene ring) |
| 7 | 1517 | 1458 | - | β C-H , C-S |
| 8 | 1539 | 1479 | 1408 | β C-H (Ani) |
| 9 | 1320 | 1269 | - | ν C=C (Ani), C-H |
| 10 | 1312-1313 | 1261-1262 | 1279 | ν C-N |
| 11 | 1207-1171 | 1160-1126 | 1167 | Cis C-H (Ani), ν C-S |
| 12 | 813- 802 | 781.5-771 | 805 | wag C-H (Thiophene ring) |
| 13 | 737-771 | 708.5-741 | 711-774 | Def (Thiophene ring), β C=C, β C-N |
| 14 | 526-548 | 506-527 | - | wag N-H, wag C-H(Ani ring) |
| 15 | 398 | - | - | H-N-H bending |

Note: ν: stretching, wag: wagging, *cis*: scissoring, β: bending, Def: deformation mod, Ani: Aniline, Tio: Tiophene.

**Table 6.** Experimental and Calculated Frequencies (in $cm^{-1}$) of PAF

| No. | Calculation frequency | | Experimental [31] | Approximate assignment |
|---|---|---|---|---|
| | Unscaled | Scaled | - | - |
| 1 | 3577 | 3439 | - | ν N-H (Ani ring) |
| 2 | 3585 | 3446 | 3475 | ν N-H (Bridging) |
| 3 | 3261-3263 | 3135-3137 | - | ν C-H (Fur ring) |
| 4 | 3170-3172 | 3047-3049 | - | ν C-H (Ani ring) |
| 5 | 1600-1674 | 1538-1609 | 1614 | ν C=C, β N-H, |
| 6 | 1545 | 1485 | - | ν C=C (Ani ring), wag C-H |
| 7 | 1587 | 1526 | - | ν C=C (Fur ring) |
| 8 | 1378-1392 | 1325-1338 | 1399 | ν C-C, sci C-H |
| 9 | 1313 | 1262 | 1245-1292[62] | ν C-$NH_2$ (Ani) |
| 10 | 1288 | 1238 | - | β C-H, N-H |
| 11 | 1200-1230 | 1154-1182 | - | ν C-O, β C-H |
| 12 | 780 | 749.8 | 780 | wag C-H (fur ring) |
| 13 | 841 | 808.5 | - | wag C-H (Ani ring) |
| 14 | 545-550 | 524-529 | 570 | wag N-H ,wag C-H |
| 15 | 332 | 319.2 | - | β N-H |

Note: ν: stretching, wag: wagging, *cis*: scissoring, β: bending, Def: deformation mod, Ani: Aniline, fur: furan.

theoretical data is for an isolated oligomer in vacuum state while the experimental is that of condensed phase. The bands at 1606-1595 $cm^{-1}$ are corresponding to N-H wagging and C=C stretching of aniline ring. The band at 1479, 1261 and 1160 $cm^{-1}$ are assigned to C-H bending, C-N stretching and C-H scissoring with 1408, 1279 and 1167 $cm^{-1}$ experimental values, respectively. The band observed at 805 $cm^{-1}$ can be attributed to C-H wagging of thiophene ring. In PAF, N-H stretching vibration can be observed at 3439 and 3446 $cm^{-1}$ near the N-H stretching of PAT. 3135 and 3047 $cm^{-1}$ bands are assigned to C-H of furan and aniline rings, respectively. The C=C stretching wave lengths of PAF are lower than those of PAT which can be attributed to its higher electronegativity. The C-N stretching is appeared at 1262 $cm^{-1}$ and N-H and C-H bending bands are appeared at 1238 $cm^{-1}$. The region of 1182-1154 $cm^{-1}$ is corresponding to C-O stretching and CH bending.

The C-H wagging of furan and aniline rings presented in 749 and 808 $cm^{-1}$, respectively, are in close agreement with 780-989 $cm^{-1}$ of experimental data [33]. The N-H stretching in PAP shifted to higher wave lengths of 3435 and 3463 $cm^{-1}$ compared to those of PAF and PAT. Asymmetric C-H of pyrrole ring is presented in region 3117- 3122 $cm^{-1}$. The 3042 $cm^{-1}$ band assigned to C-H stretching of aniline ring is presented in lower wavelengths in comparison with PAF and PAT. The band at 1608 $cm^{-1}$ is a combination of C=C, N-H and C-H wagging. The C=C band of pyrrole ring is presented at 1569 $cm^{-1}$ in higher wave length compared to

**Table 7.** Experimental and Calculated Frequencies (in $cm^{-1}$) of PAP

| No. | Calculation frequency | | Experimental [48] | Approximate assignment |
|---|---|---|---|---|
| | Unscaled | Scaled | | |
| 1 | 3573 | 3435 | - | ν N-H (Ani ring) |
| 2 | 3602 | 3463 | 3296 | ν N-H (Bridging) |
| 3 | 3242-3248 | 3117-3122 | 3052 | ν C-H (py ring) |
| 4 | 3164 | 3042 | 2934 | ν C-H (Ani ring) |
| 5 | 1673 | 1608 | - | ν C=C, N-H, wag C-H |
| 6 | 1632 | 1569 | - | ν C=C (py ring) |
| 7 | 1544 | 1484 | 1491 | β C-H |
| 8 | 1565 | 1504 | - | β C=C, C-H |
| 9 | 1305 | 1254 | 1247 | β C=C,C-N (py), β C-H |
| 10 | 1307 | 1256 | - | β C-N (Ani), β C-H |
| 11 | 1206-1209 | 1159-1162 | - | *Cis* C-H (Ani) |
| 12 | 830-840 | 797.9-807 | 840 | wag C-H (Ani ring) |
| 13 | 769 | 739.2 | 754 | wag C-H (py ring) |
| 14 | 560 | 538.3 | - | wag H-N-H |
| 15 | 510-513 | 490-493 | - | wag N-H (py ring) |
| 16 | 339-361 | 326-347 | - | C-N, C-C, Def ring |

Note: ν: stretching, wag: wagging, *cis*: scissoring, β: bending, Def: deformation mode, Ani: Aniline, Py: Pyrrole.

those of two other heterocyclic compounds.

The band about 1254 $cm^{-1}$ is assigned to the combination of C=C and C-N of pyrrole and C-H bending. The band in 1256 $cm^{-1}$ is attributed to C-N stretching of aniline which is shifted to lower wavelengths compared to that of PAT and PAF. The out of plane C-H bending of aniline and pyrrole rings are presented in about 798 and 739 $cm^{-1}$, respectively.

## CONCLUSIONS

In this work, DFT calculations were performed to investigate the structure and electronic properties of three types of co-polymers based on aniline-thiophene (PAT), aniline-pyrrole (PAP) and aniline-furan (PAF). Firstly, we proposed an oligomer model by examining the initiating and propagating reaction based on calculated local spin

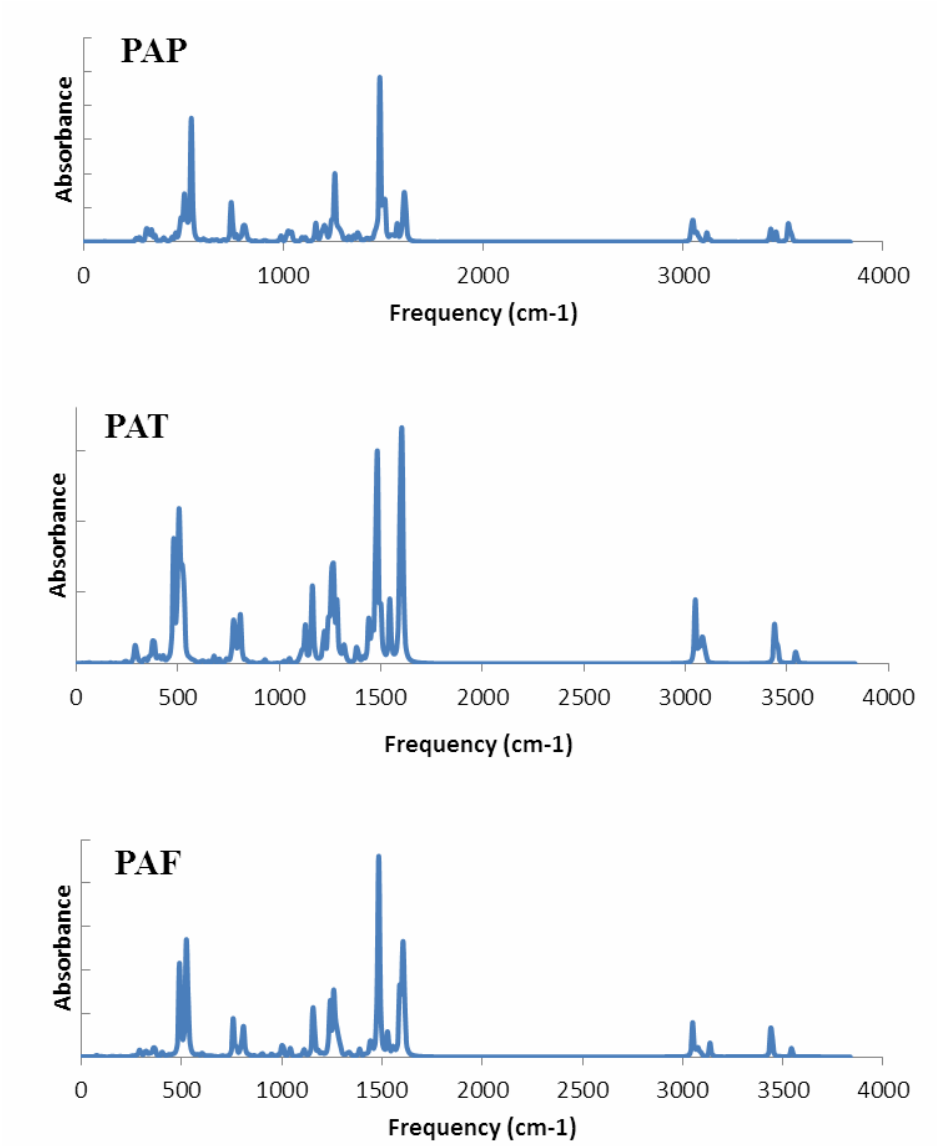


**Fig. 5.** Scaled IR spectra of PAP, PAT and PAF.

densities. The structural parameters and electronic properties like HOMO, LUMO, IP, EA and band gaps were investigated and compared with those in theoretical results. It is found that PAP has the lowest IP and EA and the most broaden band gap (3.17 eV) among the studied molecules. The values of IR spectra calculated at the same level of theory are correlated with the experimental reported values. The π-π* transition of UV-Vis spectra of PAT, PAP and PAF elevated at TD-DFT-B3LYP/6-31+G** in DMSO medium are also in good agreement with experimental reports. Among the studied molecules, PAT peaks are appeared in higher wavelengths, indicating its higher conjugation that is consistent with its lower band gap (3.21 eV).

## REFERENCES

[1] He, H.; Zhu, J.; Tao, N. J.; Nagahara, L. A.; Amlani, I.; Tsui, R., A conducting polymer nanojunction switch. *J. Am. Chem. Soc.* **2001**, *123*, 7730-7731,

DOI: 10.1021/ja016264i.

[2] Wessling, B.; Kahol, P. K.; Raghunathan, A.; McCormick, B. J., ESR and magnetic susceptibility studies of polyaniline and its blend with poly (methyl methacrylate). *Synth. Met.* **2001**, *119*, 197-198, DOI: http://dx.doi.org/10.1016/S0379-6779(00)00710-4.

[3] Yeh, J. -M.; Chen, C. -L.; Chen, Y. -C.; Ma, C. -Y.; Lee, K. -R.; Wei, Y.; Li, S., Enhancement of corrosion protection effect of poly(o-ethoxyaniline) via the formation of poly(o-ethoxyaniline)-clay nanocomposite materials. *Polymer* **2002**, *43*, 2729-2736, DOI: http://dx.doi.org/10.1016/S0032-3861(02)00005-8.

[4] Sawall, D. D.; Villahermosa, R. M.; Lipeles, R. A.; Hopkins, A. R., Interfacial polymerization of polyaniline nanofibers grafted to Au surfaces. *Chem. Mater.* **2004**, *16*, 1606-1608, DOI: 10.1021/cm0352908.

[5] Zgou, H.; Hamidi, M.; Bouachrine, M., DFT calculations of the local spin densities and oligomerization mechanism of thiophene-phenylene (TP) co-oligomers and derivatives. *J. Mol. Struct. THEOCHEM* **2007**, *814*, 25-32, DOI: http://dx.doi.org/10.1016/j.theochem.2007.02.043.

[6] Franco Jr, F. C.; Padama, A. A. B., DFT and TD-DFT study on the structural and optoelectronic characteristics of chemically modified donor-acceptor conjugated oligomers for organic polymer solar cells. *Polymer* **2016**, *97*, 55-62, DOI: http://dx.doi.org/10.1016/j.polymer.2016.05.025.

[7] Ali Shah, A. -U. -H.; Firdous, I.; Khattak, Z.; Arif, M., Efficient glucose oxidation on polyaniline film by escherichia coli with neutral red mediator. *J. Chem. Soc. Pak* **2017**, *38*, 820-826, DOI.

[8] Ali Shah, A. -U. -H.; Yasmeen, N.; Rahman, G.; Bilal, S., High electrocatalytic behaviour of Ni impregnated conducting polymer coated platinum and graphite electrodes for electrooxidation of methanol. *Electrochim. Acta* **2017**, *224*, 468-474, DOI: https://doi.org/10.1016/j.electacta.2016.12.085.

[9] Bilal, S.; Begum, B.; Gul, S.; Shah, A. -U. -H. A., PANI/DBSA/$H_2SO_4$: A promising and highly efficient electrode material for aqueous supercapacitors. *Synth. Met.* **2018**, *235*, 1-15, DOI: https://doi.org/10.1016/j.synthmet.2017.11.004.

[10] Bilal, S.; Fahim, M.; Firdous, I.; Ali Shah, A.-u.-H., Insight into capacitive performance of polyaniline/graphene oxide composites with ecofriendly binder. *Appl. Surf. Sci.* **2018**, *435*, 91-101, DOI: https://doi.org/10.1016/j.apsusc.2017.11.030.

[11] Choi, S. J.; Park, S. M., Electrochemical growth of nanosized conducting polymer wires on gold using molecular templates. *Adv. Mater.* **2000**, *12*, 1547-1549, DOI: 10.1002/1521-4095(200010)12:20<1547::AID-ADMA1547>3.0.CO;2-1.

[12] Hong, S. -Y.; Park, S. -M., Electrochemistry of conductive polymers 36. pH dependence of polyaniline conductivities studied by current-sensing atomic force microscopy. *J. Chem. Phys. B* **2005**, *109*, 9305-9310, DOI: 10.1021/jp050173g.

[13] Van Hoang, H.; Holze, R., Electrochemical synthesis of polyaniline/montmorillonite nanocomposites and their characterization. *Chem. Mater.* **2006**, *18*, 1976-1980, DOI: 10.1021/cm052707w.

[14] Zhong, W.; Liu, S.; Chen, X.; Wang, Y.; Yang, W., High-yield synthesis of superhydrophilic polypyrrole nanowire networks. *Macromolecules* **2006**, *39*, 3224-3230, DOI: 10.1021/ma0525076.

[15] Chiou, N. -R.; Lee, L. J.; Epstein, A. J., Self-assembled polyaniline nanofibers/nanotubes. *Chem. Mater.* **2007**, *19*, 3589-3591, DOI: 10.1021/cm070847v.

[16] Bilal, S.; Bibi, S.; Holze, R.; Shah, A. -U. -H. A., Structural and spectroscopic properties of homo- and Co-oligomers of *o*-phenylenediamine and *o*-toluidine: Theoretical insights compared with experimental data. *J. Chem. Phys. C* **2016**, *120*, 27141-27147, DOI: 10.1021/acs.jpcc.6b09393.

[17] Bibi, S.; Bilal, S.; Shah, A. -U. -H. A.; Ullah, H., Systematic analysis of poly(*o*-aminophenol) humidity sensors. *ACS Omega* **2017**, *2*, 6380-6390, DOI: 10.1021/acsomega.7b01027.

[18] Chiang, C. K.; Fincher, C. R.; Park, Y. W.; Heeger, A. J.; Shirakawa, H.; Louis, E. J.; Gau, S. C.;

MacDiarmid, A. G., Electrical conductivity in doped polyacetylene. *Phys. Rev. Lett.* **1977**, *39*, 1098-1101, DOI.

[19] Distefano, G.; Jones, D.; Guerra, M.; Favaretto, L.; Modelli, A.; Mengoli, G., Determination of the electronic structure of oligofurans and extrapolation to polyfuran. *J. Phys. Chem.* **1991**, *95*, 9746-9753, DOI: 10.1021/j100177a028.

[20] Libert, J.; Bredas, J. L.; Epstein, A. J., Theoretical study of \textit{p}- and \textit{n} -type doping of the leucoemeraldine base form of polyaniline: Evolution of the geometric and electronic structure. *Phys. Rev. B* **1995**, *51*, 5711-5724, DOI.

[21] Ma, J.; Wang, M.; Du, Z.; Chen, C.; Gao, J.; Xu, J., Synthesis and properties of furan-based imine-linked porous organic frameworks. *Polym. Chem*. **2012**, *3*, 2346-2349, DOI: 10.1039/C2PY20367G.

[22] Gidron, O.; Varsano, N.; Shimon, L. J. W.; Leitus, G.; Bendikov, M., Study of a bifuran vs. bithiophene unit for the rational design of [small pi]-conjugated systems. What have we learned? *Chem. Commun.* **2013**, *49*, 6256-6258, DOI: 10.1039/C3CC41795F.

[23] Ullah, H.; Ayub, K.; Ullah, Z.; Hanif, M.; Nawaz, R.; Shah, A. -U. -H. A.; Bilal, S., Theoretical insight of polypyrrole ammonia gas sensor. *Synth. Met.* **2013**, *172*, 14-20, DOI: http://dx.doi.org/10.1016/j.synthmet.2013.03.021.

[24] Ullah, H.; Shah, A. -U. -H. A.; Bilal, S.; Ayub, K., DFT Study of polyaniline $NH_3$, $CO_2$ and CO gas sensors: Comparison with recent experimental data. *J. Chem. Phys. C* **2013**, *117*, 23701-23711, DOI: 10.1021/jp407132c.

[25] Ullah, H.; Shah, A. -U. -H. A.; Bilal, S.; Ayub, K., Doping and dedoping processes of polypyrrole: DFT study with hybrid functionals. *J. Chem. Phys. C* **2014**, *118*, 17819-17830, DOI: 10.1021/jp505626d.

[26] Ammar Aouchiche, H.; Djennane, S.; Boucekkine, A., DFT study of conjugated biheterocyclic oligomers exhibiting a very low HOMO-LUMO energy gap. *Synth. Met.* **2004**, *140*, 127-133, DOI: http://dx.doi.org/10.1016/S0379-6779(03)00339-4.

[27] Johansson, E.; Larsson, S., Electronic structure and mechanism for conductivity in thiophene oligomers and regioregular polymer. *Synth. Met.* **2004**, *144*, 183-191, DOI: http://dx.doi.org/10.1016/j.synthmet.2004.03.005.

[28] Yang, S.; Olishevski, P.; Kertesz, M., Bandgap calculations for conjugated polymers. *Synth. Met.* **2004**, *141*, 171-177, DOI: http://dx.doi.org/10.1016/j.synthmet.2003.08.019.

[29] Cao, Y.; Smith, P.; Heeger, A. J., Counter-ion induced processibility of conducting polyaniline and of conducting polyblends of polyaniline in bulk polymers. *Synth. Met.* **1992**, *48*, 91-97, DOI: http://dx.doi.org/10.1016/0379-6779(92)90053-L.

[30] Wang, Z. -L.; He, X. -J.; Ye, S. -H.; Tong, Y. -X.; Li, G. -R., Design of polypyrrole/polyaniline double-walled nanotube arrays for electrochemical energy storage. *ACS Appl. Mater. Inter* **2014**, *6*, 642-647, DOI: 10.1021/am404751k.

[31] Shahhosseini, L.; Nateghi, M. R.; Kazemipour, M.; Zarandi, M. B., Electrochemical synthesis of polymer based on 4-(2-furyl) benzenamine: Electrochemical properties, characterization and applications. *Prog. Org. Coat.* **2015**, *88*, 272-282, DOI: http://dx.doi.org/10.1016/j.porgcoat.2015.07.014.

[32] Shahhosseini, L.; Nateghi, M. R.; Kazemipour, M.; Zarandi, M. B., Corrosion protective properties of poly(4-(2-Thienyl) benzenamine) coating doped by dodecyl benzene sulphonate. *Synth. Met.* **2016**, *219* (Supplement C), 44-51, DOI: https://doi.org/10.1016/j.synthmet.2016.05.006.

[33] Shahhosseini, L.; Nateghi, M. R.; SheikhSivandi, S., Electrochemical synthesis of polymer based on 4-(2-thienyl)benzenamine in aqueous solutions: Electrochemical properties, characterization and application. *Synth. Met.* **2016**, *211*, 66-74, DOI: http://dx.doi.org/10.1016/j.synthmet.2015.11.015.

[34] Li, X. -G.; Kang, Y.; Huang, M. -R., Optimization of polymerization conditions of furan with aniline for variable conducting polymers. *J. Comb. Chem.* **2006**, *8*, 670-678, DOI: 10.1021/cc060014m.

[35] Solanki, P. R.; Singh, S.; Prabhakar, N.; Pandey, M. K.; Malhotra, B. D., Application of conducting poly(aniline-co-pyrrole) film to cholesterol biosensor. *J. Appl. Polym. Sci.* **2007**, *105*, 3211-3219, DOI: 10.1002/app.26198.

[36] Özçiçek, N. P.; Pekmez, K.; Holze, R.; Yıldız, A., Spectroelectrochemical investigations of aniline-thiophene copolymers in acetonitrile. *J. Appl. Polym. Sci.* **2003**, *90*, 3417-3423, DOI: 10.1002/app.13035.

[37] Abaci, S.; Aslan, Y.; Yildiz, A., Synthesis of aniline-thiophene copolymer on β-$PbO_2$ electrode in acetonitrile. *J. Mater. Sci.* **2005**, *40*, 1163-1168, DOI: 10.1007/s10853-005-6933-1.

[38] Vogel, S.; Holze, R., Spectroelectrochemistry of intrinsically conducting aniline-thiophene copolymers. *Electrochim. Acta* **2005**, *50*, 1587-1595, DOI: http://dx.doi.org/10.1016/j.electacta.2004.10.017.

[39] Udum, Y. A.; Pekmez, K.; Yıldız, A., A new self-doped copolymer consisting of 3-methyl thiophene and aniline units. *J. Solid State Electrochem.* **2006**, *10*, 110-116, DOI: 10.1007/s10008-005-0678-2.

[40] Jensen, F., Introduction to Computational Chemistry. Wiley, 2007.

[41] Giustino, F., Materials Modelling Using Density Functional Theory: Properties and Predictions. Oxford University Press, 2014.

[42] Zhang, L.; Pei, K.; Yu, M.; Huang, Y.; Zhao, H.; Zeng, M.; Wang, Y.; Gao, J., Theoretical investigations on donor-acceptor conjugated copolymers based on naphtho[1,2-c:5,6-c]bis[1,2,5]thiadiazole for organic solar cell applications. *J. Chem. Phys. C* **2012**, *116*, 26154-26161, DOI: 10.1021/jp306656c.

[43] Sahu, H.; Panda, A. N., Computational study on the effect of substituents on the structural and electronic properties of thiophene-pyrrole-based π-conjugated oligomers. *Macromolecules* **2013**, *46*, 844-855, DOI: 10.1021/ma3024409.

[44] Zhang, L.; Yu, M.; Zhao, H.; Wang, Y.; Gao, J., Theoretical investigations on the electronic and optical characteristics of fused-ring homopolymers: Comparison of oligomer method and PBC-DFT method. *Chem. Phys. Lett.* **2013**, *570*, 153-158, DOI: http://dx.doi.org/10.1016/j.cplett.2013.03.068.

[45] Yang, L.; Feng, J. -K.; Ren, A. -M., Theoretical studies on the electronic and optical properties of two thiophene-fluorene based π-conjugated copolymers. *Polymer* **2005**, *46*, 10970-10981, DOI: http://dx.doi.org/10.1016/j.polymer.2005.09.050.

[46] Bouzzine, S. M.; Makayssi, A.; Hamidi, M.; Bouachrine, M., Bridging effect on structural and optoelectronic properties of oligothiophene. *J. Mol. Struct. THEOCHEM* **2008**, *851*, 254-262, DOI: http://dx.doi.org/10.1016/j.theochem.2007.11.023.

[47] Bhatta, R. S.; Tsige, M., Understanding the effect of heteroatoms on structural and electronic properties of conjugated polymers. *Polymer* **2015**, *56*, 293-299, DOI: http://dx.doi.org/10.1016/j.polymer.2014.11.050.

[48] Kamran, M.; Ullah, H.; Shah, A. -U. -H. A.; Bilal, S.; Tahir, A. A.; Ayub, K., Combined experimental and theoretical study of poly(aniline-co-pyrrole) oligomer. *Polymer* **2015**, *72*, 30-39, DOI: http://dx.doi.org/10.1016/j.polymer.2015.07.003.

[49] Kayi, H.; Elkamel, A., A theoretical investigation of 4,7-di(furan-2-yl)benzo[c][1,2,5]selenadiazole-based donor–acceptor type conjugated polymer. *Comput. Theor. Chem.* **2015**, *1054*, 38-45, DOI: http://dx.doi.org/10.1016/j.comptc.2014.12.011.

[50] Garcia, M.; Fomina, L.; Fomine, S., Electronic structure evolution of neutral and dicationic states of conjugated polymers with their band gap. *Synth. Met.* 2010, *160*, 2515-2519, DOI: http://dx.doi.org/10.1016/j.synthmet.2010.09.037.

[51] Brocks, G., Density functional study of polythiophene derivatives. *J. Phys. Chem.* **1996**, *100*, 17327-17333, DOI: 10.1021/jp962106f.

[52] Frisch, M. J.; Trucks, G. W.; Schlegel, H. B.; Scuseria, G. E.; Robb, M. A.; Cheeseman, J. R.; Scalmani, G.; Barone, V.; Mennucci, B.; Petersson, G. A.; Nakatsuji, H.; Caricato, M.; Li, X.; Hratchian, H. P.; Izmaylov, A. F.; Bloino, J.; Zheng, G.; Sonnenberg, J. L.; Hada, M.; Ehara, M.; Toyota, K.; Fukuda, R.; Hasegawa, J.; Ishida, M.; Nakajima, T.; Honda, Y.; Kitao, O.; Nakai, H.; Vreven, T.; Montgomery Jr., J. A.; Peralta, J. E.; Ogliaro, F.; Bearpark, M. J.; Heyd, J.; Brothers, E. N.; Kudin, K. N.; Staroverov, V. N.; Kobayashi, R.; Normand, J.; Raghavachari, K.; Rendell, A. P.; Burant, J. C.; Iyengar, S. S.; Tomasi, J.; Cossi, M.; Rega, N.; Millam, N. J.; Klene, M.; Knox, J. E.; Cross, J. B.;

Bakken, V.; Adamo, C.; Jaramillo, J.; Gomperts, R.; Stratmann, R. E.; Yazyev, O.; Austin, A. J.; Cammi, R.; Pomelli, C.; Ochterski, J. W.; Martin, R. L.; Morokuma, K.; Zakrzewski, V. G.; Voth, G. A.; Salvador, P.; Dannenberg, J. J.; Dapprich, S.; Daniels, A. D.; Farkas, Ö.; Foresman, J. B.; Ortiz, J. V.; Cioslowski, J.; Fox, D. J. Gaussian 09, Gaussian, Inc.: Wallingford, CT, USA, 2009.

[53] Dennington, R.; Keith, T.; Millam, J., GaussView, Version 5. Semichem Inc., Shawnee Mission, KS, 2009.

[54] Rosmus, P.; Bock, H.; Solouki, B.; Maier, G.; Mihm, G., Silaethene: Highly correlated wave functions and photoelectron spectroscopic evidence. *Angew. Chem. Int. Edit.* **1981**, *20*, 598-599, DOI: 10.1002/anie.198105981.

[55] Bhatta, R. S.; Tsige, M., Chain length and torsional dependence of exciton binding energies in $P_3HT$ and PTB7 conjugated polymers: A first-principles study. *Polymer* **2014**, *55*, 2667-2672, DOI: https://doi.org/10.1016/j.polymer.2014.04.022.

[56] Franco, F. C.; Padama, A. A. B., On the structural and optoelectronic properties of chemically modified oligothiophenes with electron-withdrawing substituents for organic solar cell applications: A DFT/TDDFT study. *J. Phys. Soc. Jpn.* **2017**, *86*, 064802, DOI: 10.7566/JPSJ.86.064802.

[57] Franco Jr, F. C., Computational study on the structural and optoelectronic properties of a carbazole-benzothiadiazole based conjugated oligomer with various alkyl side-chain lengths *Mol. Simul.* **2017**, *43*, 222, DOI: 10.1080/08927022.2016.1250267.

[58] McCormick, T. M.; Bridges, C. R.; Carrera, E. I.; DiCarmine, P. M.; Gibson, G. L.; Hollinger, J.; Kozycz, L. M.; Seferos, D. S., Conjugated polymers: Evaluating DFT methods for more accurate orbital energy modeling. *Macromolecules* **2013**, *46*, 3879-3886, DOI: 10.1021/ma4005023.

[59] Bouzakraoui, S.; Bouzzine, S. M.; Bouachrine, M.; Hamidi, M., Density functional theory study of conformational and opto-electronic properties of oligo-para-phenylenes. *J. Mol. Struct. THEOCHEM* **2005**, *725*, 39-44, DOI: http://dx.doi.org/10.1016/j.theochem.2005.03.050.

[60] Bouzzine, S. M.; Bouzakraoui, S.; Bouachrine, M.; Hamidi, M., Density functional theory ($B_3LYP$/6-31G*) study of oligothiophenes in their aromatic and polaronic states. *J. Mol. Struct.* **2005**, *726*, 271-276, DOI: http://dx.doi.org/10.1016/j.theochem.2005.04.023.

[61] Xu, P.; Han, X. J.; Wang, C.; Zhang, B.; Wang, H. L., Morphology and physico-electrochemical properties of poly(aniline-co-pyrrole). *Synth. Met.* **2009**, *159*, 430-434, DOI: http://dx.doi.org/10.1016/j.synthmet.2008.10.016.

[62] Ahmad, S. M.; Bibi, S.; Bilal, S.; Shah, A. -U. -H. A.; Ayub, K., Spectral and electronic properties of π-conjugated oligomers and polymers of Poly(*o*-chloroaniline-co-o-toluidine) calculated with density functional theory. *Synth. Met.* **2015**, *205*, 153-163, DOI: http://dx.doi.org/10.1016/j.synthmet.2015.04.005.